01

Raman structural analysis of polyethylene glycols: Experimental study and Quantum chemical modeling

© L.Yu. Kozlova¹, S.O. Liubimovskii¹, L.Yu. Ustynyuk², V.V. Kuzmin¹, P.V. Ivchenko², M.N. Moskovskiy³, G.Yu. Nikolaeva¹, V.S. Novikov^{1,3}

e-mail: lus.kozlowa2011@kapella.gpi.ru

Received December 26, 2024 Revised January 21, 2025 Accepted April 07, 2025

In spite of wide and diverse practical applications of polyethylene glycols (PEG), dependence of Raman spectra of these substances on molecular weight, structure of terminal groups and conformational composition is still little studied. In this work we experimentally study Raman spectra of liquid samples of ethylene glycol, tri(ethylene glycol), tetra(ethylene glycol), PEG400 and PEG600 as well as methylated mPEG550 and mPEG750. With increase in the number of PEG monomeric units the most noticeable changes are observed for wavenumbers of the bands at 321, 832 and 1125 cm⁻¹ and intensities of the bands at 885, 1043 and 1125 cm⁻¹. We showed that Raman spectra of mPEGs contain additional feature compared with the PEG spectra, namely the band at 2830 cm⁻¹. This band is related to the vibrations of O–CH₃ groups. In theoretical part of this work we analyze 16 approximations using the density functional theory for modeling the structure and Raman spectra of PEG molecules in the 7₂ helix conformation using the ethylene glycol nonamer as an example. By comparing with experimental data from Raman spectroscopy and X-ray diffraction, we show that the combination of the generalized gradient approximation functional OLYP and the 4z basis set of the of Gaussian functions type is the most suitable for calculating the structure and Raman spectra of PEG molecules.

Keywords: laser spectroscopy, Raman scattering, density functional theory, structure, conformational composition, molecular weight, polyethylene glycol, methylated polyethylene glycol.

DOI: 10.61011/EOS.2025.05.61637.32-25

Introduction

Polyethylene glycols (PEG, $HO-(CH_2-CH_2-O)_n-H$) methoxypolyethylene glycols (mPEG, $HO-(CH_2-CH_2-O)_n-CH_3)$ are widely used in many fields: in agriculture, chemical, food, pharmaceutical, cosmetic [1-5] and electronics industry [6], in solar energy [7], in archaeology [8]. One of the most important applications of PEG is their use as macro-initiators: mPEG for the synthesis of diblock copolymers or PEG for the synthesis of triblock copolymers. Such copolymers are applied to create carrier nanoparticles used in nanosomal targeted drug delivery systems with a specified release profile of the active component, and to create tissue engineering constructions in regenerative medicine [9–12]. Polyethylene glycols can be synthesized with a molecular weight (MW) in a very wide range: from hundreds to tens of millions of Daltons. The physicochemical properties of PEG strongly depend on MW, which makes it possible to precisely select PEG in accordance with the specific application [1,4,5]. The ability to modify the structure of PEG by substituting end groups with various chemically active functional groups, as well as the possibility of synthesizing branched PEG, significantly expand the scope of application of these compounds [1,2]. It is necessary

to use pure and monodisperse PEG for the production of effective and safe medicines [3,13]. Chromatography, mass spectrometry, and NMR spectroscopy methods are used to determine the MW, molecular weight distribution, and purity of PEG [3].

PEG can be in liquid, waxy, and solid states at room temperature depending on MW [1,4,5]. Two conformations of molecules in PEG semicrystalline samples are described in the literature - the helix conformation [14] and the *all-trans*-conformation [15], as well as their corresponding types of crystal lattice: monoclinic and triclinic. Using X-ray diffraction analysis, it was shown that the unit cell of the monoclinic crystal lattice contains four molecules in the conformation of a distorted helix 7₂ [14], whereas the unit cell of the triclinic crystal lattice contains one molecule in the it-trans -conformation [15]. The triclinic crystal structure is stable only in stretched films under load.

For practical applications, it is most interesting to study PEG in various medical systems in which PEG molecules are in a non-crystalline state and can adopt different conformations [1]. Vibrational spectroscopy methods are highly informative, non-destructive, and fast tools for analyzing organic compounds. However, despite the fact that attempts have been made for several decades to develop vibrational spectroscopy methods for quantitative analysis

¹ Prokhorov General Physics Institute of the Russian Academy of Sciences, Moscow, Russia

² Chemistry Department, M.V. Lomonosov Moscow State University, Moscow, Russia

³ Federal Scientific Agronomic and Engineering Center VIM, Moscow, Russia

of the conformational composition of PEG, this task still remains unresolved [16–24]. The main problem is the large number of possible conformations of molecules in the noncrystalline state [6,25]. Therefore, despite the accumulated knowledge about the vibrational spectra of PEG, at present the method of Raman spectroscopy is not used for routine analysis of PEG in various systems and materials. In this regard, the development of methods for determining the content, structure and conformational composition of PEG molecules in a non-crystalline state in systems of complex structure is relevant.

The methods of quantitative analysis of the structure of a substance or mixture of substances using Raman spectroscopy are based on attributing Raman bands to certain vibrations of atomic nuclei and determining the dependence of the wavenumbers and intensities of Raman bands on the structural characteristics of the substance under study. When examining a series of samples with different MW of molecules, the structure of end groups, the degree of branching or conformational composition, it is possible to find the dependence of the spectral characteristics of the bands on these structural characteristics. These problems can be solved by numerical methods, for example, by modeling using the density functional theory (DFT).

Calculations based on quantum chemistry methods, including calculations by the DFT method, have been effectively used for many years to determine the structure and vibrational spectra of various organic molecules and molecular systems. Currently, a number of commercial and non-commercial programs have been created that allow calculations for polyatomic molecules to be performed with high accuracy and with low cost of computing resources. However, it is necessary to choose the best approximation for obtaining reliable and practically important results: a combination of the electron density functional and a basis set of wave functions. Nowaday, several hundred different functionals and basis sets have been proposed, combinations of which are selected for each specific task.

In our recent study [26], the structures and Raman spectra of a PEG molecule with 9 monomeric units in two conformations were calculated using the OLYP/4z approximation: the conformation of helix 72 and the trans-conformation. Based on comparison with experimental Raman spectra, it was shown that liquid and solid PEG substances at room temperature are in the most energetically favorable conformation - the conformation of helix 7_2 . same time, the content of PEG molecules in the alltrans-conformation is insignificant in comparison with the most probable conformation, both according to estimates using the energy values of molecules obtained by the DFT method, and according to the results of comparing the calculated and experimental Raman spectra. Based on calculations of the structure and Raman spectra of ethylene glycol (EG) oligomers in the conformation of helix 7_2 , it was determined that the positions of the peaks of the PEG Raman lines around 830, 1100, and 1470 cm⁻¹ should strongly depend on the length of the molecule.

There are several papers [6,27–30], devoted to the modeling of EG oligomers using DFT. However, short oligomers were considered in [6,28-30], the lengths of which are insufficient to describe the structure of the molecule in the conformation of helix 7_2 . Only in [27] the results of calculations by the DFT method in the B3LYP/6-31G approximation for the EG oligomer with 8 monomeric units in the conformation of helix 72 with methoxy and methyl groups at the ends of the chain are presented. In comparison with the X-ray diffraction data from [14], the authors obtained a good match for the period of regularity of helix 72, however, the torsion angles in the molecular backbone did not correspond well to the experimental data from [14]. The authors explained this result by the fact that the calculations were carried out for a single chain (an isolated structure), while in the crystal lattice the PEG chains are distorted due to intermolecular interaction.

However, we have previously shown that the widely used hybrid B3LYP functional poorly describes both the structure and the Raman spectra of various organic molecules, such as the normal alkanes [31] and polylactide [32], while the generalized gradient functional OLYP gives a better match for both substances. At the same time, selection of the best DFT approximation for calculating the structure and Raman spectra was not carried out for PEG. Therefore, one of the tasks of this work was to determine the best combination in terms of compliance with experimental data for calculating the structure and Raman spectra of PEG..

16 approximations of DFT are used in this work: 4 electron density functionals (OLYP [33], PBE [34], B3LYP [35] and PBE0 [36]) and 4 basis sets of Gaussian type functions (3z and 4z [37], cc-pVTZ and cc-pVQZ [38]). The modeling is performed for the EG oligomer in the conformation of helix 7₂ with 9 monomeric units, i.e. for the EG nonamer. The comparison is performed with the experimental Raman spectra of PEG with MW of 400 Da, which corresponds to approximately 9 monomeric units.

The choice of the four functionals under consideration is attributable to the following reasons. The generalized gradient functional OLYP was chosen by us to calculate the structure and Raman spectra of normal alkanes in [31] and poly(L-lactide) in [32] and has since been successfully used by us to model the structure and Raman spectra of organic compounds of different classes [26,39,40]. The generalized gradient functional PBE and the hybrid functionals B3LYP and PBE0 are among the most common and frequently used functionals for modeling the structure and properties of large molecules and molecular systems. In addition, there is a clear pairwise relationship between the functionals of different classes OLYP — B3LYP and PBE PBE0, consisting in a significant pairwise similarity of the correlation parts of these functionals, which allows us to identify common patterns in the transition from generalized gradient functionals to hybrid ones.

The selected basis sets of Gaussian type functions have successfully proven themselves earlier in the study of the

Liquid samples							
Sample designation	Molecular weight, Da Approximate number of PEG monomeric units		c Manufacturer				
EG	62	1	Sigma-Aldrich				
TriEG	150	3	ACMEC				
TetraEG	194	4	ACMEC				
PEG400	400*	9	Standard TS 20.16.40-007-71150986-2019				
mPEG550	550*	12	Sigma-Aldrich				
PEG600	600^{*}	13	MIFCT				
mPEG750	750*	16	Sigma-Aldrich				

Table 1. EG oligomers under study

Note. * Here and further: Average MW.

spectral properties of various molecular systems [26,32,39–46]. The basis sets of functions 3z and 4z [37] use the same exponential values for different angular momenta [47]. The correlation consistent basis sets cc-pVTZ and cc-pVQZ are widely used for quantum chemical calculations and are constructed taking into account all polarization functions that lower energy by an order of magnitude.

This construction is balanced and consistent from the point of view of taking into account the change (decrease) in the energy of the molecule in accordance with the contributions of functions with different values of angular momenta. In addition, the 3z basis set is dimensionally comparable to the cc-pVTZ set, and the 4z basis set is comparable to the cc-pVQZ set. Based on this, it is appropriate to conduct a study with extended basis sets, which can be compared with each other both in terms of type of construction and dimension.

Thus, the objectives of this study are: (1) selection of the best approximation (a combination of the electron density functional and a basis set of wave functions) for calculating the structure and Raman spectra of PEG, (2) experimental study of the Raman spectra of PEG and mPEG with different MW in the liquid state using the results of calculations of Raman spectra by the DFT method for interpreting the results.

Samples and methods

Samples

In the course of this work, commercial samples of EG and EG oligomers with different MW were experimentally studied. Methylated PEGs (mPEGs) are distinguished by the presence of the attached group CH₃, which substitutes the hydrogen atom. At room temperature all the samples were in a liquid state. The characteristics of the samples are presented in Table 1. The purity of the samples varies from 98.0 to 99.5%.

Modeling by the DFT method

For accomplishing the task of this work we performed a quantum chemical modeling of the structure and Raman spectra of the EG oligomer with 9 monomeric units (EG nonamer), adopted the conformation of helix 7₂, which we previously identified as the most probable for PEG in both solid and liquid states [26]. A structure with 9 monomeric units was chosen for modeling, so that there was one PEG monomeric unit with terminal fragments H or OH on both sides of the fragment of helix 7₂. The two edge monomeric units may have geometric distortions relative to other units of the helix 7₂ Therefore, they had to be added at the edges of the EG oligomer.

The modeling was performed on the basis of DFT. We used the program "PRIRODA" [48], performed calculations in the approximation of the gas phase (isolated molecule), and considered atomic vibrations as vibrations of a system of uncoupled harmonic oscillators. In order to establish optimal combinations of functional and basis set from the point of view of comparison with experimental data, calculations were carried out using 4 electron density functionals and 4 basis sets. We used the generalized gradient functionals OLYP [33] and PBE [34], as well as the hybrid functionals B3LYP [35] and PBE0 [36]. The contracted basis sets of Gaussian type functions 3z and 4z [37] implemented in the program "PRIRODA" were used as basis sets, as well as the contracted correlation consistent basis sets ccpVTZ and cc-pVQZ [38]. Thus, we modeled the structure and Raman spectra of the EG nonamer in 16 different approximations within the framework of the DFT. A more detailed description of the calculation procedure and the approach we use to broaden the peaks in the calculated Raman spectra is presented in [31].

After obtaining all sets of vibration wavenumbers and Raman activities in 16 approximations, the calculated bands were broadened using the self-made program Broadened Spectrum Modeling [49]. The weighting coefficient between the Gauss and Lorentz functions was determined from the deconvolution of the spectra and is 0.5. The following values of full width at half maximum were selected: $60 \, \mathrm{cm}^{-1}$ for

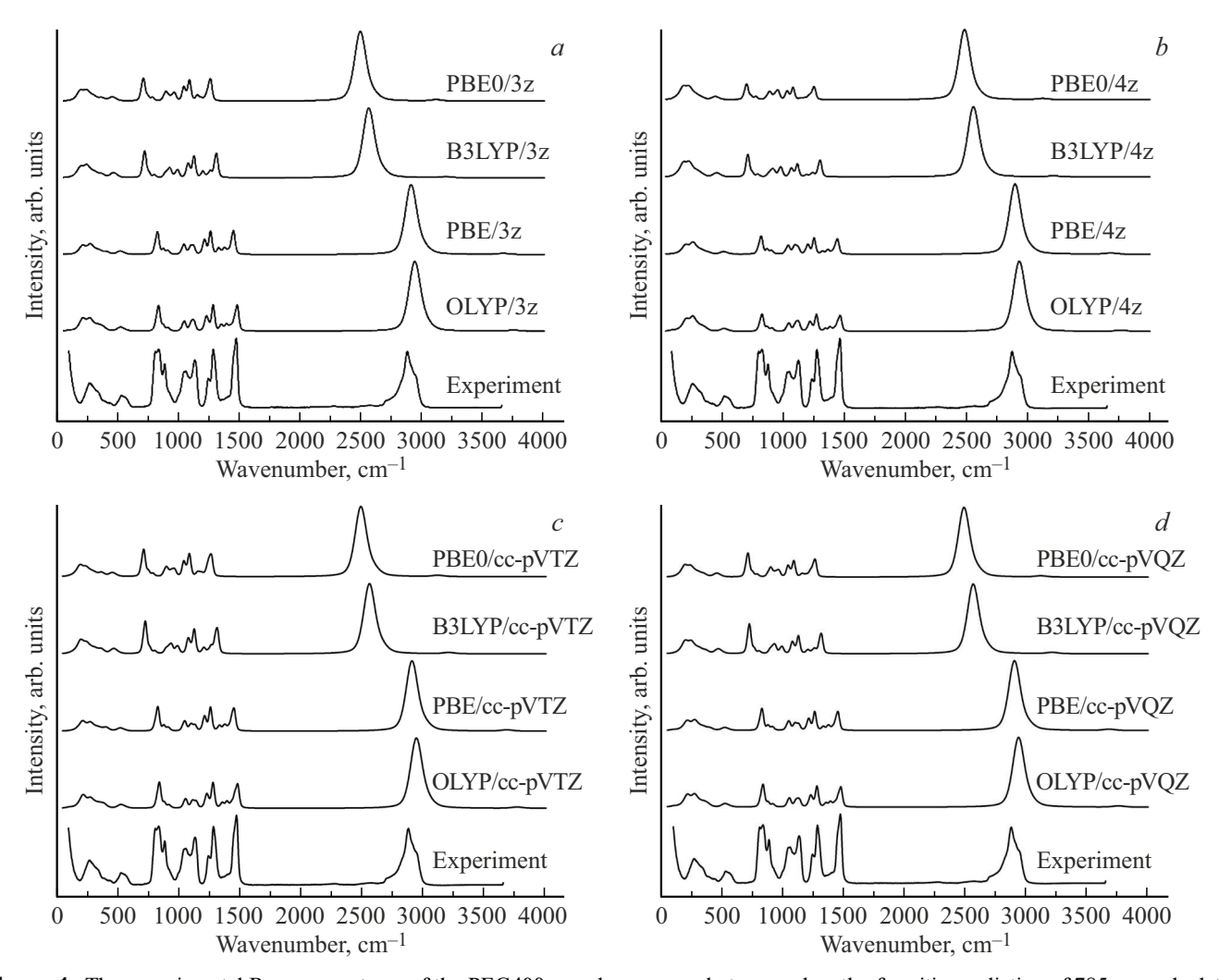


Figure 1. The experimental Raman spectrum of the PEG400 sample, measured at a wavelength of exciting radiation of 785 nm, calculated and broadened Raman spectra of the EG nonamer, obtained using the electron density functionals OLYP, PBE, B3LYP and PBE0 and the following basis sets: 3z(a), 4z(b), cc-pVTZ(c), cc-pVQZ(d).

the bands in the spectral range up to $600\,\mathrm{cm^{-1}}$, $30\,\mathrm{cm^{-1}}$ for the bands in the spectral range of $700-1500\,\mathrm{cm^{-1}}$ and $110\,\mathrm{cm^{-1}}$ for the bands in the spectral range of $2400-3800\,\mathrm{cm^{-1}}$. The spectrum of the PEG400 sample with an average MW of 400 Da, approximately corresponding to 9 PEG monomeric units, was used as a reference experimental Raman spectrum.

Raman spectroscopy

The Raman spectra of all samples were recorded at room temperature using a Senterra II confocal Raman microscope (Bruker Optics, USA). The following instrumental parameters were used to record the spectra: scattering by 180° , spectral resolution of $4\,\mathrm{cm}^{-1}$, excitation wavelengths of $532\,\mathrm{nm}$ (with laser radiation power of $25\,\mathrm{mW}$) and $785\,\mathrm{nm}$ (with $100\,\mathrm{mW}$ laser radiation power). The exciting and scattered radiation was focused by a lens with a magnification of $20\times$ (numerical aperture of 0.40). The diameter of

the laser spot on the sample surface in the case of using the excitation wavelength of $532\,\mathrm{nm}$ was $10\,\mu\mathrm{m}$, and in the case of wavelength of $785\,\mathrm{nm}$ was $12\,\mu\mathrm{m}$.

Results and discussion

Theoretical

Figure 1 shows a comparison of the reference experimental Raman spectrum of the PEG400 sample with the calculated and broadened Raman spectra of the EG nonamer obtained in the considered 16 theoretical approximations. We have found that the choice of the electron density functional affects the calculated spectrum to a much greater extent than the choice of the basis set of the wave functions. It should be noted that in the case of measurements on the Raman microscope used by us at an excitation wavelength of 785 nm, the sensitivity of the detector decreases with increasing wavelength of

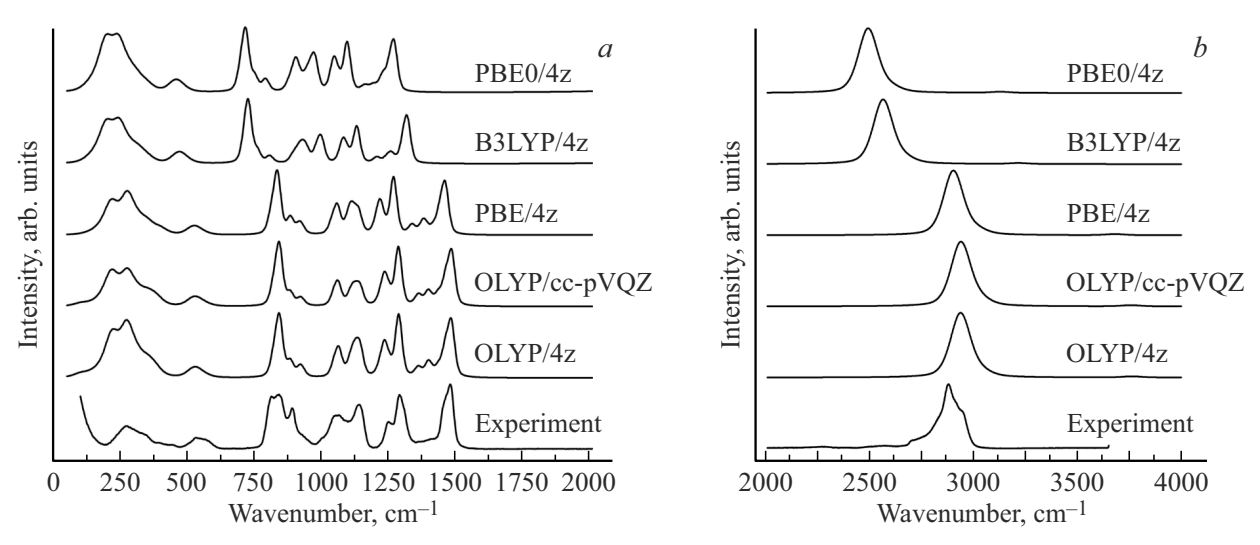


Figure 2. Experimental Raman spectrum of the PEG400 sample measured at a wavelength of exciting radiation of 785 nm, calculated and broadened Raman spectra of the EG nonamer in the approximations OLYP/4z, OLYP/cc-pVQZ, PBE/4z, B3LYP/4z and PBE0/4z: the spectral ranges of 100-2000 (a), $2000-4000 \, \mathrm{cm}^{-1} (b)$.

the detectable radiation. Therefore, in the experimental Raman spectrum of the PEG400 sample in Fig. 1, the intensity of the lines in the spectral range after 2500 cm⁻¹ is underestimated in comparison with the intensity of the lines in the spectral range from 100 to 1500 cm⁻¹.

To select the best approximation from the 16 considered options, the wavenumbers of the 5 most intense and well-resolved Raman lines in the reference experimental spectrum and in the calculated spectra of the EG nonamer in the spectral range of 700–1500 cm⁻¹ were compared. This comparison showed that calculations using the generalized gradient functionals OLYP and PBE describe the experimental spectrum significantly better than calculations using the hybrid functionals B3LYP and PBE0. average difference between the calculated and measured wavenumbers for the five bands under consideration in the case of the B3LYP functional exceeded 140 cm⁻¹, and in the case of the PBE0 functional exceeded 170 cm⁻¹. In the case of the PBE functional, the average wavenumber difference was significantly smaller and, depending on the choice of the basis set, was $18-20\,\mathrm{cm}^{-1}$. The best agreement with the experimental data was in the case of the OLYP functional: the average wavenumber difference, depending on the choice of the basis set, was $4-9 \,\mathrm{cm}^{-1}$. The best match to the experimental spectrum was in the case of combinations of the OLYP functional with basis sets of 4z (average wavenumber difference is 4 cm⁻¹, the maximum difference between the compared wavenumbers is $10\,\mbox{cm}^{-1})$ and cc-pVQZ (average wavenumber difference is 5 cm⁻¹, the maximum difference between the compared wavenumbers is 12 cm⁻¹). Taking into account the errors of both measurements and quantum chemical modeling, it can be concluded that the combinations of OLYP/4z and OLYP/cc-pVQZ reproduce the experimental Raman spectra of oligomers with comparable accuracy. Bearing in mind

the results we obtained for PLA in [32], the OLYP/4z approximation has additional advantages for calculating the Raman spectra of PEG, since it can be further used to carry out calculations for PLA-PEG copolymers widely used for medical purposes.

Fig. 2 shows a more detailed comparison of the experimental spectrum with the theoretical ones for combinations of all the functionals used in the work with a basis set of 4z, as well as for the OLYP/cc-pVQZ approximation.

The OLYP/4z approximation reproduces better than other approximations considered not only the experimental Raman spectra of the PEG400, but also the structure of PEG molecules. Table 2 shows the calculated geometric characteristics of the EG nonamer and their experimental values obtained by X-ray diffraction for high-molecular-weight PEG in [14]. The numbering of atoms is shown in Fig. 3.

The dihedral angles obtained by the DFT method are compared with the average values of the angles determined using X-ray diffraction, since for the PEG molecule in the conformation of helix 7_2 the values of the dihedral angles in the crystal lattice relative to C-O bonds vary from -185.9 to -155.7° , and the values of the dihedral angles relative to the C-C bonds vary in the range from 49.0 to 91.8° . The experimental values of the angles vary in such a significant range, since attributable to intermolecular interactions in the crystal lattice, the structure of PEG molecules in the conformation of helix 7_2 is distorted relative to the structure of PEG in this conformation outside any environment [14].

The period of regularity of helix 7_2 in the case of all the theoretical approximations under consideration turns out to be longer than in the experiment, which can be explained, among other things, by the limitations of the model used in the calculations: as the length of oligomeric chain increases,

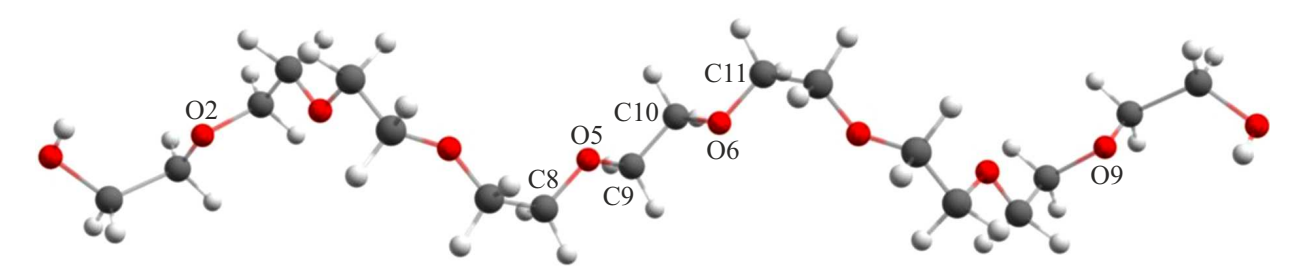


Figure 3. The structure of the EG nonamer, optimized in the OLYP/4z approximation. Carbon atoms are shown in grey, hydrogen atoms are shown in white, oxygen atoms are shown in red.

Table 2. The period of regularity of helix 7_2 and dihedral angles in the center of the backbone of the EG nonamer, calculated in all considered 16 approximations "density functional-basis set", in comparison with experimental data

Method $l(O_2-O_9)$		$\angle (C_8 - C_5 - C_9 - C_{10}), \text{ deg}$	$\angle (O_5 - C_9 - C_{10} - O_6), deg$	$\angle (C_9 - C_{10} - O_6 - C_{11}), \text{ deg}$		
Experiment	19.48	-174.0*	68.4*	-174.0*		
OLYP/3z	19.78	-177.1	73.2	-177.1		
OLYP/4z	19.84	-177.3	74.0	-177.3		
OLYP/cc-pVTZ	19.64	-177.3	73.2	-177.3		
OLYP/cc-pVQZ	19.80	-176.8	73.7	-176.8		
PBE/3z	19.88	-176.5	74.2	-176.3		
PBE/4z	19.84	-176.9	74.3	-176.9		
PBE/cc-pVTZ	19.88	-176.8	75.0	-176.8		
PBE/cc-pVQZ	19.91	-176.4	74.8	-176.5		
B3LYP/3z	20.99	-176.7	75.6	-176.7		
B3LYP/4z	21.04	-177.1	76.1	-177.0		
B3LYP/cc-pVTZ	20.92	-177.5	76.4	-177.7		
B3LYP/cc-pVQZ	21.06	-176.9	76.7	-176.9		
PBE0/3z	21.03	-177.1	75.0	-177.1		
PBE0/4z	21.13	-177.3	75.5	-177.5		
PBE0/cc-pVTZ	21.11	-177.5	76.4	-177.5		
PBE0/cc-pVQZ	21.20	-177.0	76.5	-176.9		

Note. * The experimental values of the dihedral angles relative to the C-O- and C-C-bonds obtained by X-ray diffraction are presented here as their average values [14].

the period of regularity of the helix should decrease. Nevertheless, for the OLYP functional in combination with any basis set, the overestimation of the value of this parameter relative to the experimental data is no more than 2%. A comparable, though slightly larger, overestimation occurs when using another generalized gradient functional, PBE. In the case of the hybrid B3LYP and PBE0 functionals, the relative overestimation of the regularity period of helix 7_2 ranges from 7-9%, i.e. increases by several times. It is worth noting that a direct comparison of the dihedral angles in the backbone of an EG nonamer calculated in the

gas phase approximation with the dihedral angles measured using X-ray diffraction in a crystal lattice is not fully correct. Due to the strong distortion of the geometry of helix 7_2 [14], the comparison is only of an estimative nature.

Thus, when comparing the 4 electron density functionals under consideration, it is the OLYP functional that best describes the structural parameters of PEG molecules. The choice of a basis set from 4 considered options has little effect on the calculation of geometric characteristics, and, therefore, the combination of the OLYP functional and the

basis set of 4z is quite suitable for calculating the structure of PEG.

Experimental

In accordance with the technical capabilities of the commercial Raman microscope used, the Raman spectra of EG and EG oligomers were recorded in the range from 45 to 4270 cm⁻¹ for the wavelength of exciting radiation of 532 nm and 55 to 3650 cm⁻¹ for a wavelength Two regions turned out to be the most informative ranges of the PEG Raman spectrum: from 100 to 1800 cm⁻¹ (the so-called "fingerprint" region, hereinafter range I, Fig. 4, a, b) and range of $2250-4250 \,\mathrm{cm}^{-1}$ (hereinafter range II, Fig. 5, a, b). Raman bands of the studied samples were not found in the range from 1800 to 2250 cm⁻¹. For the convenience of processing and analyzing the spectra, both ranges were considered separately. After subtracting the fluorescence background, the intensity in the spectra in the range I was normalized to the peak intensity of the most intense band in the range of $1400-1500\,\mathrm{cm}^{-1}$, and in the range II — to the peak intensity of the band with a wavenumber of about $2878 \, \text{cm}^{-1}$.

When comparing the Raman spectra recorded at excitation by radiation with different wavelengths, two things must be taken into account. Firstly, when using radiation with a wavelength of 785 nm, the sensitivity of the detector used decreases significantly with increasing wavelength of the detectable radiation. This leads to an underestimation of the intensity of the Raman bands in the range II compared to the range I. As a result, the band of the stretching vibrations of OH bonds, which has a noticeable intensity in the spectra recorded with exciting radiation with a wavelength of 532 nm, is reduced in intensity when recording spectra with exciting radiation with a wavelength of 785 nm.

Secondly, non-polarized Raman spectra were recorded in this work, i.e. without the use of an analyzer. In the case of registration of non-polarized Raman spectra, the direction of polarization of the scattered light relative to the direction of polarization of the exciting radiation differs for the two excitation wavelengths, and this leads to differences in the relative intensities of the Raman bands.

Fig. 4 and 5 show that the Raman spectra of the EG oligomers change monotonously with increasing molecule length, and the trends are the same for both wavelengths of the exciting radiation. As expected, the strongest changes are observed for short oligomers.

For a reliable analysis of the structure of EG oligomers using Raman spectra, it is necessary to select Raman bands, the wavenumber or intensity of which varies significantly with increasing length of the molecule. Such Raman bands of EG oligomers are predominantly localized in the range I — the "fingerprint region" (Fig. 4, a, b): the strongest changes in wavenumber are observed for the lines around 321, 832 and $1125 \, \mathrm{cm}^{-1}$ (Table 3), and the

Table 3. Dependence of wavenumbers of PEG Raman bands on MW

	Compound	Molecular weight, Da	Wavenumber, cm ⁻¹						
			785 nm			532 nm			
	EG	62	347	_	1	346	-	ı	
	TriEG	150	321	832	1125	317	831	1123	
	TetraEG	194	297	834	1130	289	834	1129	
	PEG400	400	269	837	1133	275	834	1133	
	mPEG550	550	273	846	1137	269	844	1134	
	PEG600	600	274	840	1134	274	837	1135	
	mPEG750	750	278	845	1136	273	844	1136	

strongest changes in intensity are observed for the lines around 885, 1043, and $1125\,\mathrm{cm^{-1}}$ (Table 4). Here and further, the wavenumbers of the Raman bands are indicated for triethylene glycol (TriEG).

Range $50-400 \, \text{cm}^{-1}$

A narrow band corresponding to the longitudinal acoustic mode LAM [50,51] is observed in the Raman spectra of crystalline PEG in the region of 10-50 cm⁻¹, and its counterpart which is a wide and having complex structure D-LAM (disordered longitudinal acoustic mode) band is observed in the spectra of liquid and amorphous PEG in the region of $200-400 \,\mathrm{cm}^{-1}$ [52]. The D-LAM band is a superposition of bands corresponding to vibrations of molecules in various conformational states. These two bands have been studied quite well. In particular, it is known that the wavenumbers of both the bands LAM [50] and D-LAM [52] shift into the low-wavenumber range with increasing length of the molecule. The wavenumber of LAM depends on the type of end groups (PEG or mPEG) [50]. Since crystalline samples are not studied in this work, only the D-LAM band will be discussed further.

The shape and position of the D-LAM band strongly depend on the length of the oligomer (Fig. 4, *a*, *b*, Table 3). The EG spectrum is characterized by a symmetrical peak, the maximum of which is at a wavenumber of 347 cm⁻¹. The D-LAM band becomes much wider in the PEG spectra and its shape becomes asymmetrical. The D-LAM wavenumbers for the two excitation wavelengths are slightly different. This is probably attributable to the fact that when the spectra are excited by radiation with a wavelength of 532 nm, the intensity of the D-LAM band is much lower, and as a result, the wavenumber measurement error is much greater.

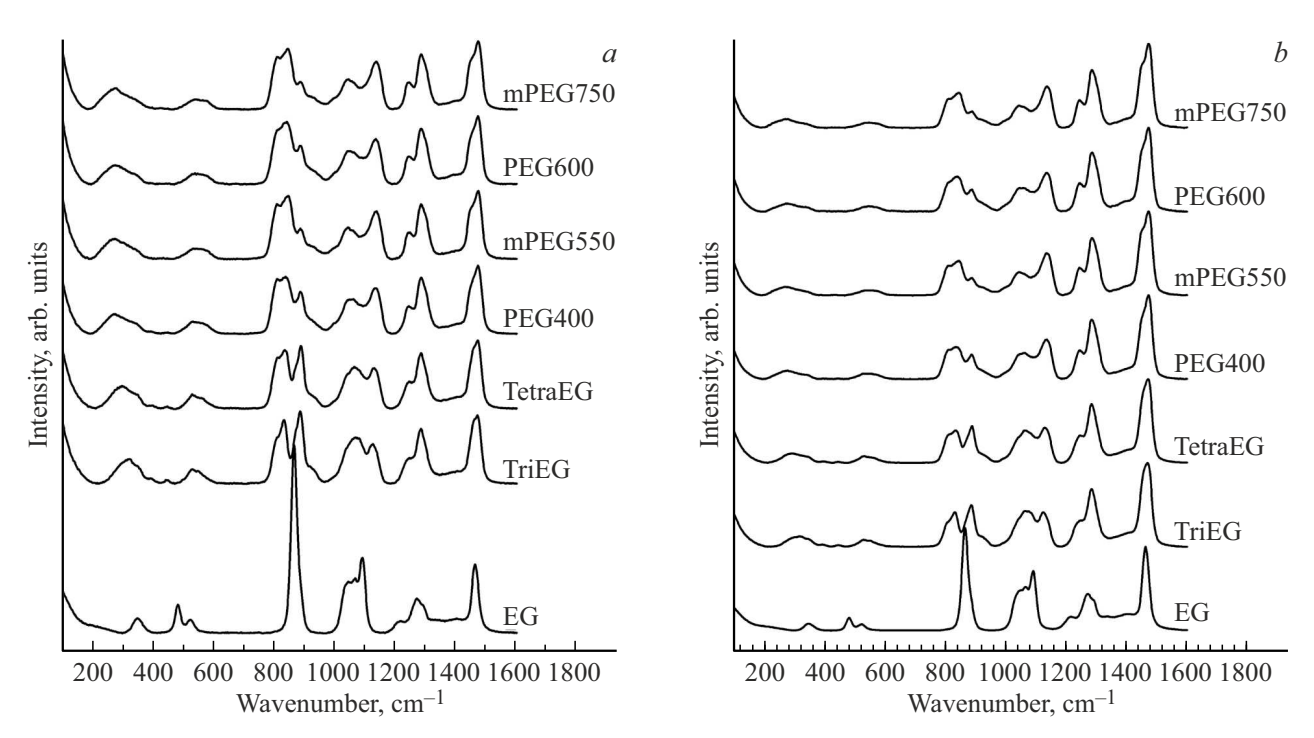


Figure 4. Raman spectra of EG, PEG, and mPEG recorded at excitation wavelengths of 785 (a) and 532 nm (b), range I.

Compound	Molecular weight, Da	I_{885}/I_{1472}		I_{1043}/I_{1472}		I_{1125}/I_{1472}		I_{3431}/I_{2878}	
		532	785	532	785	532	785	532	785
EG	62	_	-	-	_	-	-	0.18	_
TriEG	150	1.06	0.50	0.67	0.43	0.58	0.41	0.08	-
TetraEG	194	0.92	0.44	0.61	0.39	0.59	0.42	0.05	_
PEG400	400	0.62	0.29	0.50	0.31	0.67	0.47	0.03	_
mPEG550	550	0.44	0.21	0.46	0.27	0.70	0.50	0.02	_
PEG600	600	0.56	0.26	0.48	0.28	0.66	0.46	0.04	_
mPEG750	750	0.40	0.19	0.44	0.26	0.70	0.49	0.02	-

Table 4. Dependence of the ratio of peak intensities of the PEG Raman bands on MW

Range 800-900 cm⁻¹

The Raman spectrum in the range from 800 to 900 cm⁻¹ changes significantly with increasing the oligomer length (Fig. 4, *a*, *b*, Table 3): the wavenumber of the band at about 832 cm⁻¹ increases noticeably, and the intensity of the band at about 885 cm⁻¹ decreases considerably. These observations fully correspond to the results of calculations by the DFT method presented in [26]. In addition, the bands in this range change significantly in the experimental Raman spectra at transition from liquid oligomers to solid ones [26,53]. The Raman bands in this area are closely located to each other and therefore poorly resolved. This makes it difficult to analyze these bands.

The quantum chemical modeling carried out in this work has shown that the band at about 832 cm⁻¹ refers to a superposition of the symmetric stretching vibrations of C-O-C-bonds and the rocking vibrations of groups CH₂. The results of calculating the Raman spectra of EG oligomers in the conformation of helix 7₂ with the number of the monomeric units from 2 to 13 [26] showed that the wavenumber of this band increases with increasing number of the monomeric units in the helix. This band is observed at a wavenumber of 844 cm⁻¹ in experimental spectra of solid PEG. Based on theoretical and experimental studies, the authors of several papers also attributed this band to vibrations of molecules in the conformation of helix 7₂ [53].

In particular, the authors of [30] carried out measurements of the Raman spectra of solid mPEG with MW

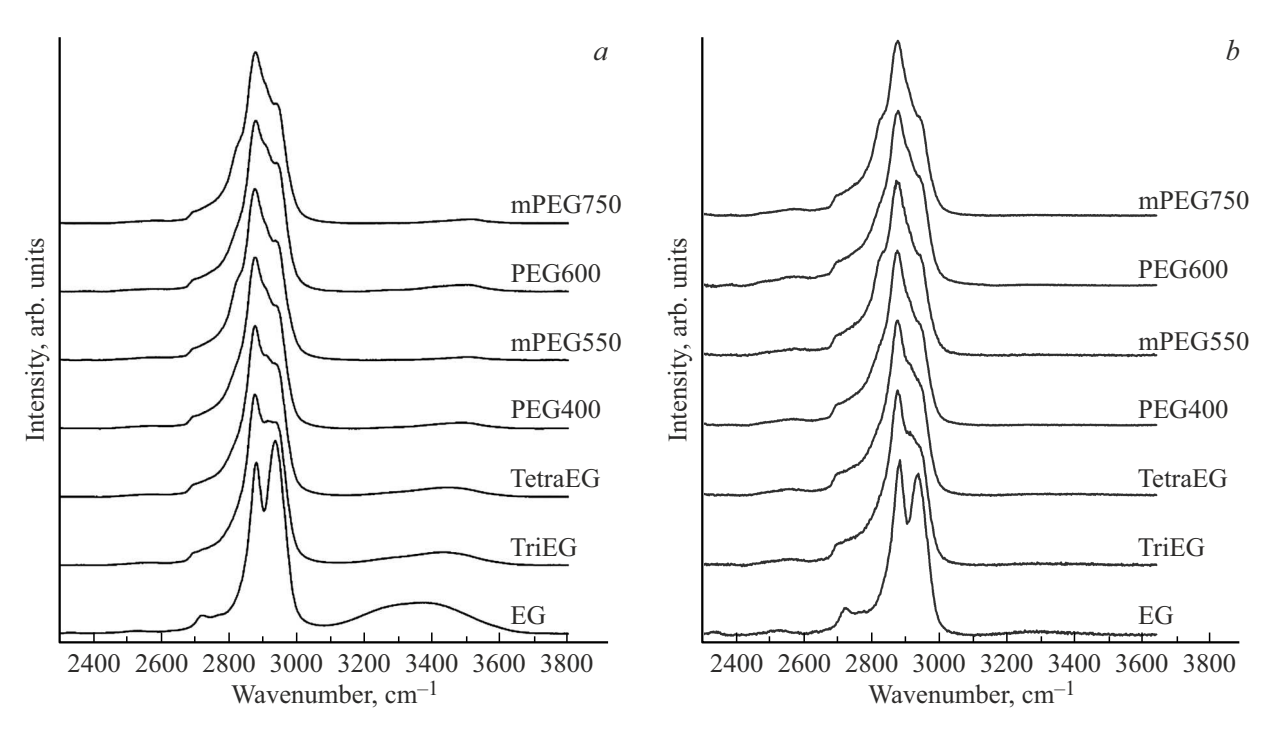


Figure 5. Raman spectra of EG, PEG, and mPEG recorded at excitation wavelengths of 532 (a) and 785 nm (b), range II.

of 1000 Da with the increase in temperature. Based on the deconvolution of the spectra in the range from 750 to 975 cm⁻¹ using 9 components, they concluded that two peaks at 810 and 844 cm⁻¹, obtained as a result of spectrum deconvolution, correspond to vibrations of the monomeric units in *gauche*- and *trans*-conformations relative to the C–O bond, respectively. The authors showed that with the increase in temperature, the intensity of the band at 810 cm⁻¹ increases, and the intensity of the band at 844 cm⁻¹ decreases, indicating a decrease in the content of molecules in the conformation of helix 7₂.

According to the DFT modeling, the band at 885 cm⁻¹ relates to the symmetric stretching vibrations of C-C-Obonds at the edges of the oligomer. It is stated in [19] that there is a band corresponding to the stretching vibration of the terminal group C-OH in the Raman spectra of low-molecular-weight PEG. Modeling of EG oligomers of different lengths [26] showed that the position of the band at 885 cm⁻¹ does not change significantly with increasing length of the molecule, but the intensity sharply decreases. This band is not present in the experimental Raman spectra of solid PEG [26], which confirms that it relates to the vibrations at the edges of the molecule. In addition, as it will be shown below, the intensity of this band in the mPEG spectra is lower than in the PEG spectra, which also proves its assignment to the vibrations at the edges of non-methylated oligomers.

The authors of a number of papers [53] reported the appearance of a weak and wide band at $880 \, \mathrm{cm}^{-1}$ in the spectra of solid PEG upon heating or in solutions. This band relates to vibrations of molecules in disordered

conformations [19] and is not associated with the band at 885 cm⁻¹, which corresponds to the vibrations at the edges of the molecule.

For a more detailed interpretation of the Raman spectra in the region of $800-900\,\mathrm{cm^{-1}}$, it is necessary to calculate the Raman spectra of EG oligomers of various lengths and in various conformations. However, based on the already available data, it can be concluded that the wavenumber and intensity of the band at $832\,\mathrm{cm^{-1}}$ can be used to estimate the length of the molecule and conformational composition, respectively, and the intensity of the band at $885\,\mathrm{cm^{-1}}$ can be used for estimating the length of the molecule.

Range 1000-1200 cm⁻¹

The spectral range from 1000 to 1200 cm⁻¹ contains two Raman bands that strongly depend on the length of the molecule: a wide and having complex structure band with a peak at 1043 cm⁻¹, the intensity of which decreases with the increase in the length of the molecule, and a band at 1125 cm⁻¹, for which a shift towards higher wavenumbers and an increase in intensity are observed with the increase in the oligomer length.

Our modeling of the EG oligomer in the conformation of helix 7₂ with 9 monomeric units showed that there are a number of quite intense bands in this range, for which the dependence on the length of the oligomer should be different. In particular, the band at 1040 cm⁻¹ was attributed to the asymmetric stretching vibrations of C–C–O-bonds at the edges of the oligomer. The decrease in the intensity of this band with an increase in the length of the molecule is explained by a decrease in the relative contribution of

vibrations of the edge sections of the molecule to the Raman spectrum of the oligomer. Four bands corresponding to backbone vibrations are also calculated in the range from 1050 to $1065\,\mathrm{cm^{-1}}$: two bands corresponding to the superposition of the stretching vibrations of C–C-bonds and scissoring vibrations of C–C-bonds, and two bands corresponding to the superposition of the stretching vibrations of C–C-bonds and the symmetric stretching vibrations of C–O-C-bonds.

Indeed [26,53], a broad band with a peak of $1045 \,\mathrm{cm}^{-1}$, is observed in the experimental Raman spectra of liquid PEG, and a rather narrow band with a peak of 1060 cm⁻¹ is observed in the spectra of solid PEG, instead of a band with a peak of 1045 cm⁻¹. This suggests that the intensity of a band at 1040 cm⁻¹ corresponding to the asymmetric stretching vibrations of C-C-O-bonds at the edges of the oligomer decreases with the increase in the oligomer length, and only bands, which are related to vibrations of the molecular backbone, remain in the Raman spectrum of solid PEG. However, it is reported in [18,19] that a band at 1045 cm⁻¹ appears in the Raman spectrum of the melt and aqueous solution of solid PEG6000. The authors suggested that this band relates to disordered conformations of molecules. We believe that this band may indeed correspond to vibrations of molecules in conformations, which differ from the conformation of helix 7₂. Nevertheless, in order to accurately assign bands in this range, it is necessary to calculate the Raman spectra of EG oligomers of different lengths and in different conformations.

The wavenumber and intensity of the band at 1125 cm⁻¹ change significantly with the increase in the oligomer length. The experimentally observed wavenumber shift fully corresponds to the results of calculations of the Raman spectra of EG oligomers in the conformation of helix 7₂ [26]. Based on the results of our modeling, the band at 1125 cm⁻¹ was attributed to a superposition of the asymmetric stretching of C–O–C- and scissoring C–C–O-vibrations of the molecule in the conformation of helix 7₂. This conclusion coincides with the conclusions of [30], in which, according to the results of a study of the Raman spectrum of PEG1000 at heating, the band at 1125 cm⁻¹ was also attributed to vibrations of molecules in the conformation of helix 7₂.

However, the Raman spectrum in this range has a very complex structure. In accordance with the results of our quantum chemical modeling, other 7 quite intense bands are observed in the range from 1100 to 1140 cm⁻¹, which represent superpositions of the stretching vibrations of C–O–C-bonds, stretching vibrations of C–C-bonds and deformation vibrations of C–C-O-bonds in different proportions. Additional calculations are required to assign bands in this range more accurately.

Range 2500-4000 cm⁻¹

In the Raman spectra of EG oligomers recorded at a wavelength of exciting radiation of 532 nm, there is a

noticeable band of stretching vibrations of OH bonds. The intensity of this band decreases with an increase in MW of the oligomer (Table 4). This result is explained by a decrease in the number of OH terminal groups compared to the number of the monomeric units in the oligomer as the length of the oligomer increases. In addition, the intensity of this band in the mPEG spectra is lower than in the PEG spectra. Therefore, the intensity of the band of the stretching vibrations of OH bonds can be used as an additional source of information about the length of the molecule and the structure of the terminal groups.

The spectral range from 2250 to 3100 cm⁻¹ (Fig. 5, *a, b*) is less informative than the "fingerprint" region, because of the strong overlapping of PEG Raman bands. In this range, the bands of the symmetric (at 2880 cm⁻¹) and asymmetric (at 2900 cm⁻¹) stretching vibrations of groups CH₂, as well as overtones and combination tones of vibrations from the "fingerprint" region are observed. With an increase in the length of the oligomer, the intensity of the shoulder at 2930 cm⁻¹ decreases monotonously.

However, the most interesting result is the presence of a shoulder at about $2830~\rm cm^{-1}$ in the mPEG spectra compared to the PEG spectra. This spectral feature is clearly observed in the mPEG spectra recorded when the spectra are excited by radiation with both a wavelength of $532~\rm nm$ and a wavelength of $785~\rm nm$. It belongs to the vibrations of the group $O-CH_3$ [54]. Thus, an additional shoulder at $2830~\rm cm^{-1}$ can be used for identification of PEG and mPEG by Raman spectroscopy.

Conclusions

The best approximation of the DFT was determined in the theoretical part of this study for calculating the structures and Raman spectra of PEG. For this purpose, combinations of generalized gradient (OLYP, PBE) and hybrid (B3LYP, PBE0) electron density functionals with basis sets of Gaussian type functions (3z, 4z) and correlation consistent basis sets (cc-pVTZ, cc-pVQZ) were analyzed.

It has been found that both the Raman spectra and the geometric parameters of PEG molecules are worst described by the hybrid functionals B3LYP and PBE0, and best described by the generalized gradient functional OLYP. The influence of the choice of the basis set on the calculation results turned out to be significantly less than the influence of the choice of the functional. The OLYP/4z and OLYP/cc-pVQZ approximations provide the structure and Raman spectra of PEG closest to the experimental ones. Earlier, we obtained good results for one of these approximations (OLYP/4z) and longer PEG chains in [26]. This allows hoping for the successful use of this approximation for both solid and liquid PEG, as well as for PEG copolymers with other polymers, in particular biodegradable ones.

The Raman spectra of liquid commercial samples EG, TriEG, TetraEG, PEG400, mPEG550, PEG600 and mPEG750 were studied in the experimental part of this

paper. It is shown that the Raman spectra of EG oligomers change monotonously with increasing molecular length, regardless of the wavelength of the exciting radiation. The strongest changes with an increase in the number of PEG monomeric units are observed for the wavenumbers of the bands at 321, 832, and $1125 \, \mathrm{cm}^{-1}$, as well as for the intensities of the bands at 885, 1043, and $1125 \, \mathrm{cm}^{-1}$. These dependencies can be used to estimate the length of the PEG molecules and their conformational composition.

It was found that there is a shoulder near 2830 cm⁻¹ in the Raman spectra of mPEG, compared with the PEG spectra. This band belongs to the vibrations of the group O–CH₃ and can be used to identify short PEG and mPEG by Raman spectroscopy.

A number of bands, which also depend on MW of EG oligomers, were not analyzed, since their analysis requires deconvolution of the spectra on individual components. Such an analysis should be carried out on the basis of quantum chemical calculations of the Raman spectra of EG oligomers, which will allow determining the number of lines in a certain spectral range, their relative intensities and depolarization ratios.

The study of a larger set of samples of methylated PEG, primarily short oligomers, is required to establish the exact dependence of the Raman spectra on the type of end groups (group OH or the group $O-CH_3$). This will confirm the differences in the intensities of a number of PEG and mPEG bands in the "fingerprint" region and the appearance of an additional band near $2830\,\mathrm{cm}^{-1}$.

Thus, the study shows that Raman spectroscopy in combination with quantum chemical calculations is a promising method for analyzing the structure and conformational composition of PEG molecules. In order to further develop Raman spectroscopy methods, it is necessary to calculate the Raman spectra of EG oligomers of various lengths and in various conformations. This will make it possible to separate the contributions to changes of the Raman spectra from changes in the length of the molecule and from changes in the conformational composition of the molecules and reliably interpret the Raman spectra of PEG, in which there is a strong overlapping of a large number of bands. However, based on the data already available, it can be concluded that the analysis of the PEG Raman spectra makes it possible to estimate the MW and conformational composition of liquid PEG, as well as to distinguish between PEG and mPEG.

Conflict of interest

The authors declare that they have no conflict of interest.

References

- [1] A.A. D'souza, R. Shegokar. Expert Opin. Drug Deliv., 13, 1257-1275 (2016). DOI: 10.1080/17425247.2016.1182485
- [2] D. Hutanu. Mod. Chem. Appl., **02**, (2014). DOI: 10.4172/2329-6798.1000132

- [3] C. Bento, M. Katz, M.M.M. Santos, C.A.M. Afonso. Org. Process Res. Dev., 28, 860–890 (2024). DOI: 10.1021/acs.oprd.3c00428
- [4] K.R. Santhanakrishnan, J. Koilpillai, D. Narayanasamy. Cureus, **16**, (2024). DOI: 10.7759/cureus.66669
- [5] A. Servesh, S. Lokesh Kumar, S. Govindaraju, S. Tabassum, J. Raj Prasad, N. Kumar, S.G. Ramaraj. Polym. Adv. Technol., 35, 1–13 (2024). DOI: 10.1002/pat.6433
- [6] R.T. Rooney, K.G. Schmitt, H.F. von Horsten, R. Schmidt,
 A.A. Gewirth. J. Electrochem. Soc., 165, D687-D695 (2018).
 DOI: 10.1149/2.0581814jes
- [7] X. Xu, Y. Sun, W. Wang, L. Ju, R. Shu, H. Gu. J. Energy Storage, 104, 114581 (2024). DOI: 10.1016/j.est.2024.114581
- [8] M.N. Mortensen, H. Egsgaard, S. Hvilsted, Y. Shashoua,
 J. Glastrup. J. Archaeol. Sci., 34, 1211–1218 (2007).
 DOI: 10.1016/j.jas.2006.10.012
- [9] Y. Puchkova, N. Sedush, E. Kuznetsova, A. Nazarov,
 S. Chvalun. Rev. Adv. Chem., 13, 152–159 (2023).
 DOI: 10.1134/s2634827623600056
- [10] E.V. Kuznetsova, N.G. Sedush, Y.A. Puchkova, S.V. Aleshin, E.V. Yastremsky, A.A. Nazarov, S.N. Chvalun. Polymers (Basel), 15, 2296 (2023). DOI: 10.3390/polym15102296
- [11] Y.A. Puchkova, N.G. Sedush, A.D. Ivanenko, V.G. Shuvatova, G.A. Posypanova, S.N. Chvalun. Mendeleev Commun., 33, 404–407 (2023). DOI: 10.1016/j.mencom.2023.04.033
- [12] Y.A. Kadina, E. V. Razuvaeva, D.R. Streltsov, N.G. Sedush, E.V. Shtykova, A.I. Kulebyakina, A.A. Puchkov, D.S. Volkov, A.A. Nazarov, S.N. Chvalun. Molecules, 26, 1–15 (2021). DOI: 10.3390/molecules26030602
- [13] J. Hu, S. Liu. Curr. Opin. Biomed. Eng., 24, 100419 (2022). DOI: 10.1016/j.cobme.2022.100419
- [14] Y. Takahashi, H. Tadokoro. Macromolecules, 6, 672–675 (1973). DOI: 10.1021/ma60035a005
- [15] Y. Takahashi, I. Sumita, H. Tadokoro. J. Polym. Sci. Part A-2, 11, 2113–2122 (1973). DOI: 10.1002/pol.1973.180111103
- [16] M. Kozielski, M. Mühle, Z. Błaszczak, M. Szybowicz. Cryst. Res. Technol., 40, 466–470 (2005). DOI: 10.1002/crat.200410368
- [17] M. Kozielski. J. Mol. Liq., 128, 105–107 (2006). DOI: 10.1016/j.molliq.2005.12.012
- [18] H. Matsuura, K. Fukuhara. J. Mol. Struct., 126, 251–260 (1985). DOI: 10.1016/0022-2860(85)80118-6
- [19] H. Matsuura, K. Fukuhara. J. Polym. Sci. Part B, 24, 1383–1400 (1986). DOI: 10.1002/polb.1986.090240702
- [20] S. Di Fonzo, B. Bellich, A. Gamini, N. Quadri, A. Cesáro. Polymer (Guildf), 175, 57–64 (2019). DOI: 10.1016/j.polymer.2019.05.004
- [21] E. Talebian, M. Talebian. Optik (Stuttg)., **125**, 228–231 (2014). DOI: 10.1016/j.ijleo.2013.06.095
- [22] L. Malysheva, Y. Klymenko, A. Onipko, R. Valiokas,
 B. Liedberg. Chem. Phys. Lett., 370, 451–459 (2003).
 DOI: 10.1016/S0009-2614(03)00116-7
- [23] L. Koenig, A.C. Angood. J. Polym. Sci. Part A-2, **8**, 1787–1796 (1970). DOI: 10.1002/pol.1970.160081013
- [24] R. Majumdar, K.S. Alexander, A.T. Riga. Pharmazie, 65, 342–346 (2010). DOI: 10.1691/ph.2010.9280
- [25] X. Yang, Z. Su, D. Wu, S.L. Hsu, H.D. Stidham. Macro-molecules, 30, 3796—3802 (1997). DOI: 10.1021/ma961804v
- [26] V.V. Kuzmin, V.S. Novikov, L.Y. Ustynyuk, K.A. Prokhorov, E.A. Sagitova, G.Y. Nikolaeva. J. Mol. Struct., 1217, 128331 (2020). DOI: 10.1016/j.molstruc.2020.128331

- [27] M. Kobayashi, H. Sato. Polym. J., 40, 343-349 (2008). DOI: 10.1295/polymj.PJ2007140
- [28] M. Kozlowska, J. Goclon, P. Rodziewicz. ChemPhysChem, 17, 1143-1153 (2016). DOI: 10.1002/cphc.201501182
- [29] M. Naganathappa, A. Chaudhari. Vib. Spectrosc., 95, 7–15 (2018). DOI: 10.1016/j.vibspec.2017.12.006
- [30] A.Z. Samuel, S. Umapathy. Polym. J., 46, 330-336 (2014). DOI: 10.1038/pj.2014.10
- [31] S.M. Kuznetsov, V.S. Novikov, E.A. Sagitova, L.Y. Ustynyuk, A.A. Glikin, K.A. Prokhorov, G.Y. Nikolaeva, P.P. Pashinin. Laser Phys., 29, 085701 (2019). DOI: 10.1088/1555-6611/ab2908
- [32] S.O. Liubimovskii, L.Y. Ustynyuk, V.S. Novikov, K.T. Kalinin, N.G. Sedush, S.N. Chvalun, S.V. Gudkov, M.N. Moskovskiy, G.Y. Nikolaeva. Phys. Wave Phenom., 32, 423–430 (2024). DOI: 10.3103/S1541308X24700420
- [33] J. Baker, P. Pulay. J. Chem. Phys., 117, 1441-1449 (2002). DOI: 10.1063/1.1485723
- [34] J.P. Perdew, K. Burke, M. Ernzerhof. Phys. Rev. Lett., 77, 3865–3868 (1996). DOI: 10.1103/PhysRevLett.77.3865
- [35] R.H. Hertwig, W. Koch. Chem. Phys. Lett., **268**, 345–351 (1997). DOI: 10.1016/S0009-2614(97)00207-8
- [36] C. Adamo, V. Barone. J. Chem. Phys., **110**, 6158–6170 (1999). DOI: 10.1063/1.478522
- [37] D.N. Lajkov. Razvitie ekonomnogo podhoda k raschetu molekul metodom funkcionala plotnosti i ego primenenie k resheniyu slozhnyh himicheskih zadach. Avtoref. kand. dis. (MGU im. M.V. Lomonosova, M., 2000) (in Russian).
- [38] T.H. Dunning. J. Chem. Phys., **90**, 1007–1023 (1989). DOI: 10.1063/1.456153
- [39] V.S. Novikov, V.V. Kuzmin, S.M. Kuznetsov, M.E. Darvin, J. Lademann, E.A. Sagitova, L.Y. Ustynyuk, K.A. Prokhorov, G.Y. Nikolaeva. Spectrochim. Acta Part A, 255, 119668 (2021). DOI: 10.1016/j.saa.2021.119668
- [40] V.V. Kuzmin, V.S. Novikov, E.A. Sagitova, L.Y. Ustynyuk, K.A. Prokhorov, P.V. Ivchenko, G.Y. Nikolaeva. J. Mol. Struct., 1243, 130847 (2021). DOI: 10.1016/j.molstruc.2021.130847
- [41] S.M. Kuznetsov, V.S. Novikov, G.Y. Nikolaeva, M.N. Moskovskiy, P.K. Laptinskaya, E.A. Sagitova. Doklady Physics, 520 (1), 32–40 (2025). DOI: 10.31857/S26867400250105e3
- [42] S.M. Kuznetsov, M.S. Iablochnikova, E.A. Sagitova, K.A. Prokhorov, G.Y. Nikolaeva, L.Y. Ustynyuk, P.V. Ivchenko, A.A. Vinogradov, A.A. Vinogradov, I.E. Nifant'ev. Polymers (Basel), 12, 2153 (2020). DOI: 10.3390/polym12092153
- [43] S.M. Kuznetsov, E.A. Sagitova, K.A. Prokhorov, D.I. Mendeleev, G.Y. Nikolaeva, L.Y. Ustynyuk, A. Materny, P. Donfack. Spectrochim. Acta Part A, 282, 121653 (2022). DOI: 10.1016/j.saa.2022.121653
- [44] D.D. Vasimov, A.A. Ashikhmin, M.A. Bolshakov, M.N. Moskovskiy, S.V. Gudkov, D.V. Yanykin, V.S. Novikov. Doklady Physics, Technical Sciences, 513, 10–17 (2023). DOI: 10.31857/S2686740023060147
- [45] V.V. Kuzmin, S.M. Kuznetsov, V.S. Novikov, L.Yu. Ustynyuk, P.V. Ivchenko, G.Yu. Nikolaeva, E.A. Sagitova. Results Chem., 7, 101293 (2024). DOI: 10.1016/j.rechem.2023.101293
- [46] S.O. Liubimovskii, L.Y. Ustynyuk, A.N. Tikhonov. J. Mol. Liq., 333, 115810 (2021). DOI: 10.1016/j.molliq.2021.115810
- [47] D.N. Laikov. Chem. Phys. Lett., 281, 151–156 (1997). DOI: 10.1016/S0009-2614(97)01206-2
- [48] D.N. Laikov, Y.A. Ustynyuk. Russ. Chem. Bull., 54, 820–826 (2005). DOI: 10.1007/s11172-005-0329-x

- [49] V.S. Novikov, V.V. Kuzmin, M.E. Darvin, J. Lademann, E.A. Sagitova, K.A. Prokhorov, L.Y. Ustynyuk, G.Y. Nikolaeva. Spectrochim. Acta Part A, 270, 120755 (2022). DOI: 10.1016/j.saa.2021.120755
- [50] S. Krimm, K. Song. Macromolecules, 23, 1946-1957 (1990).DOI: 10.1021/ma00209a012
- [51] I. Kim, S. Krimm. Macromolecules, 29, 7186-7192 (1996).DOI: 10.1021/ma960331p
- [52] F. Migliardo, S. Magazú, M.T. Caccamo. J. Mol. Struct., 1048, 261–266 (2013). DOI: 10.1016/j.molstruc.2013.05.060
- [53] E.A. Sagitova, K.A. Prokhorov, G.Y. Nikolaeva, A.V. Baimova, P.P. Pashinin, A.Y. Yarysheva, D.I. Mendeleev. J. Phys. Conf. Ser., 999, 012002 (2018). DOI: 10.1088/1742-6596/999/1/012002
- [54] A. Espina, S. Sanchez-Cortes, Z. Jurašeková. Molecules, **27**, 1–17 (2022). DOI: 10.3390/molecules27010279

Translated by A.Akhtyamov